DEMONSTRATION OF THE HOLLOW CHANNEL PLASMA WAKEFIELD ACCELERATOR*

S. J. Gessner[1] †, J. M. Allen, C. Clarke, J.P. Delahaye, J. Frederico, S. Green, C. Hast,
M.J. Hogan, N. Lipkowitz, M. Litos, B. O'Shea, D. Walz, V. Yakimenko, G. Yocky,
SLAC National Accelerator Laboratory, Menlo Park, CA, USA
W. An, C. Clayton, C. Joshi, K. Marsh, W. Mori, N. Vafaei-Najafabadi,
University of California, Los Angeles, CA, USA
E. Adli, C. A. Lindstrom, University of Oslo, Oslo, Norway
S. Corde, A. Doche, Ecole Polytechnique, Saclay, France
W. Lu, Tsinghua University, Beijing, China
[1]also at Stanford University, Stanford, CA, USA

Abstract

Over the past decade, there has been enormous progress in the field of beam and laser-driven plasma acceleration of electron beams. However, in order for plasma wakefield acceleration to be useful for a high-energy e^+e^- collider, we need a technique for accelerating positrons in plasma as well. This is a unique challenge, because the plasma responds differently to electron and positron beams, with plasma electrons being pulled through the positron beam and creating a non-linear focusing force that is disruptive to the beam. Here, we demonstrate a technique called hollow channel acceleration that symmetrizes the wakefield response to beams of either charge. Using a transversely shaped laser pulse, we create an annular plasma with a fixed radius of 200 µIm. We observe the acceleration of a positron bunch with energies up to 33.4 MeV in a 25 cm long channel, indicating an effective gradient greater than 100 MeV/m. This is the first demonstration of a technique that way be used for staged acceleration of positron beams in plasma.

INTRODUCTION

Hollow channel plasmas have been theorized as a solution for accelerating positrons in plasma without deleterious transverse forces [1–3]. Wakes in the hollow channel are created by a driving positron (or electron) beam propagating through the channel. The beam excites a longitudinal mode that has an accelerating phase behind the drive beam. A trailing positron beam (called the witness) can be located in this region of the wake where it will be accelerated. If both the driving and trailing beams are well-aligned, there are no transverse forces acting on the beams and their emittances are preserved.

Here, we describe our technique for creating the hollow channel plasma as well as a novel method for determining the shape of the plasma channel by measuring its influence on the trajectory of the positron beam. We demonstrate for the first time the acceleration of a witness positron bunch in a hollow channel plasma wakefield and compare our results

to theoretical calculations and numerical particle in cell simulations.

EXPERIMENTAL SETUP

The experiment was carried out at the FACET beamline at SLAC National Accelerator Laboratory [4]. FACET is the first facility that combines all of the ingredients needed for a proof-of-principle hollow channel plasma wakefield experiment, namely, an intense positron beam, a terawatt-class laser, and a plasma source. Our plasma source is a lithium vapor produced in a heat-pipe oven with variable number density from $n_0 = 0.1$ to $3 \times 10^{17}\,\mathrm{cm}^{-3}$ and variable length. The density and length of the lithium vapor is controlled by adjusting the temperature of the oven heaters and pressure of the helium buffer gas [5]. The experimental setup is depicted in Figure 1.

Laser

The FACET 800 nm, Ti:sapphire laser delivered 100 fs FWHM laser pulses with 10–100 mJ per pulse to the lithium oven [6]. The laser pulse is synchronized with the arrival time of the positron beam such that the laser ionizes the channel 3±0.25 ps before the beam arrives. The laser is focused into the lithium vapor resulting in a plasma channel that is 0 to 70 cm long, depending on the setup of the oven and the longitudinal position of the kinoform optic, which is controlled by a delay stage. For the experiments where acceleration was observed, the channel length was 25 cm.

Optics

The laser acquires a high-order Bessel profile by passing through a kinoform, which imprints a phase pattern on the laser. The kinoform is a 1 mm thick piece of fused silica with an etched pattern that approximates the ideal phase

$$\Phi = k_\perp r + m\phi \tag{1}$$

to create a high-order Bessel profile, where r and ϕ are the radial and azimuthal coordinates, m is the Bessel order, and $k_\perp$ is the transverse wavenumber [7–9]. The resulting laser intensity is

$$I(r, z) = \eta I_0 2\pi k z \sin(\alpha)^2 J_7^2(k_\perp r), \tag{2}$$

10 Opening, Closing and Special Presentations

04 Prize Presentation

with η the first-order diffraction efficiency, measured to be 96%. Here, $I_0 \approx 1 \times 10^{10}$ W/cm^2 is the incident laser intensity. This intensity pattern produces a transverse, high-order Bessel pattern that does not change over the length of the focus (see Figure 2). This is important because it allows us to create a hollow channel plasma with a constant radius over its many cm-long length.

Positron Beam

The positron beam has a mean energy of 20.35 GeV at the end of the FACET linac. We use beams with low numbers of positrons per bunch, typically less than 5×10^9, to avoid beam-ionization of lithium. The particle beam is brought to a focus near the start of the plasma channel with β_x^* and β_y^* of 1 m and 5 m, respectively. The plasma channel is much shorter than β^*, so the beam size is nearly constant over the length of the channel. The focal spot of the beam is about $\sigma_x \approx \sigma_y \approx 50\,\mu$m. The bunch length is variable, with a longer "two-bunch" setup used to put a witness positron bunch in the accelerating phase of the wake.

Two-Bunch Generation

When operating in two-bunch mode, the positron beam enters the final bunch compressor with a correlated energy spread, or chirp. After the first bend of the chicane, at a point of maximum horizontal dispersion and minimum β_x, a system of collimators is used to selectively transmit portions of the energy spectrum [10]. This translates into longitudinal
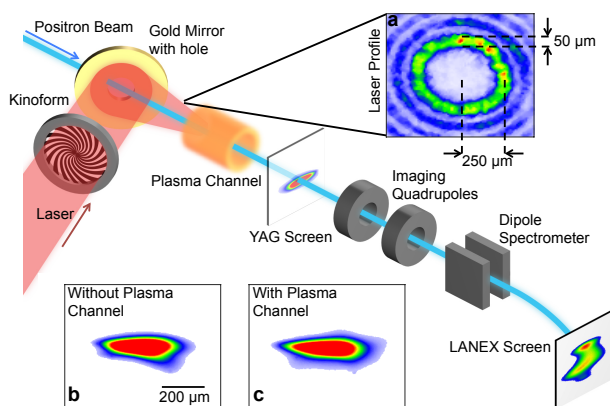

Figure 1: Schematic of the experiment. The laser passes through the kinoform and is coupled to the beam axis by a gold mirror with a small central hole. Inset a) shows the laser profile upstream of the lithium oven. A scintillating YAG screen 1.95 m downstream of plasma is used to measure the positron beam profile. Inset b) shows the positron beam spatial profile as imaged on the YAG screen with the laser off and no plasma present. Inset c) shows the beam profile with the laser on when the positron beam propagates through the plasma channel. The two profiles are similar, indicating that there are no net focusing forces due to the plasma channel. A scintillating Lanex screen downstream of the dipole measures the beam energy spectrum.
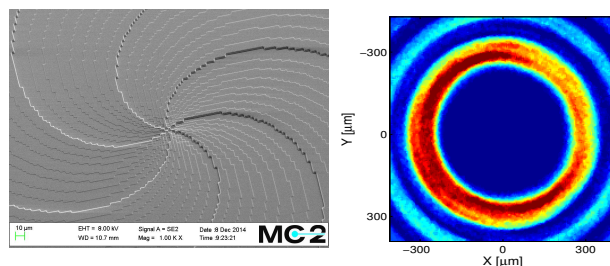

Figure 2: Left: Scanning electron microscope image of the center of an $m = 6$ kinoform showing the 6 spiral arms. Right: The intensity pattern of the high-order Bessel focus 60 cm downstream of the kinoform optic.

collimation as well due to the chirp, with the high-energy particles forming the drive beam and the low-energy particles forming the witness beam. For the experiments where acceleration was observed, the average populations of the drive and witness bunches were 1.6×10^9 and 1.6×10^8 positrons, respectively.

Spectrometers

We use two spectrometers to measure the energy change of the positron drive and witness beams due to the wakefield. The first spectrometer is downstream of the collimation system and upstream of the interaction region. The spectrometer in non-destructive and records the beam energy spectrum on a shot-to-shot basis. The second spectrometer is downstream of the interaction region. It is an imaging spectrometer, composed of the two quadrupoles and a vertical dipole, and can distinguish changes to the beam energy from changes to the beam orbit. The spectrometer was adjusted to image the end of the hollow channel plasma for the low-energy witness beam, such that the transfer matrix element from the channel to the spectrometer screen was zero (i.e. $R_{34} = 0$) for these particles. The resolution of our spectrometer is roughly 3 MeV. The final energy recorded by the downstream spectrometer is corrected for shot-to-shot energy jitter using the upstream spectrometer, which is critical for measuring the small changes to the beam energy expected from the hollow channel wakefield.

THEORY AND SIMULATION

In our experiment, we limit the charge of positron bunches in order to avoid ionization of the on-axis lithium vapor. Using a low-charge drive beam, we excite linear modes of the hollow channel plasma. In this case 'linear' means that the impulse due to the drive beam is not large enough to significantly displace the plasma electrons from their initial positions in the wall of the channel. The hollow channel plasma is thus acting as dielectric waveguide with

$$\varepsilon = 1 - \frac{\omega_p^2}{\omega^2} < 0, \tag{3}$$

where ε is the permittivity of the plasma, which depends on the plasma frequency ω_p and the frequency of the acceler-

ating mode ω. For this geometry, the accelerating modes are only supported for frequencies $\omega < \omega_p$. Therefore ε is less than zero. This implies that the fields decay rapidly to zero in the annular plasma boundary, so the plasma provides good confinement for the fields.

Using the approach described in Chao Chapter 2 [11], we can determine the single-particle wake function and convolve it with the beam distribution to find the net field experienced by the positron bunch. For the $m = 0$, accelerating mode driven by an ultrarelativistic beam ($v_\phi = c$), the longitudinal wake function is

$$W_z(r, \xi) = \frac{\mathcal{G} k_p^2}{\pi \epsilon_0} \cos(\chi k_\mathrm{p} \xi), \qquad (4)$$

where k_p is the plasma wavenumber and $\xi = z - ct$ is the co-moving coordinate. Note that $W_z(r, \xi)$ has no dependence on r; the wake is uniform across the channel. $\mathcal{G}$ and χ are geometric quantities related to the wake amplitude and wavelength, respectively, and are determined by the inner radius a and outer radius b of the plasma annulus

$$\chi = \sqrt{\frac{2B_1}{2B_1 + k_p a B_0}}, \qquad (5)$$

$$\mathcal{G} = \frac{B_0}{k_p a (2B_1 + k_p a B_0)}, \qquad (6)$$

with

$$B_0 = K_0(k_p a) I_0(k_p b) - K_0(k_p b) I_0(k_p a), \qquad (7)$$
$$B_1 = K_1(k_p a) I_0(k_p b) + K_0(k_p b) I_1(k_p a), \qquad (8)$$

where I_n and K_n are the modified Bessel functions. The functions B_0 and B_1 arise from matching the boundary conditions of the fields at the inner and outer radii of the plasma annulus. Plugging in our experimental parameters ($a = 200\,\mu\mathrm{m}$, $b = 280\,\mu\mathrm{m}$, $n_0 = 2.5 \times 10^{16}\,\mathrm{cm}^{-3}$, $k_p = 0.3\,\mu\mathrm{m}^{-1}$) we calculate the wavelength to be $400\,\mu\mathrm{m}$ with a single-particle wake amplitude of $0.1\,\mathrm{V/m}$. Note that the single-particle wake amplitude scales as a^{-2}, so we can achieve significantly larger accelerating fields by using a narrower plasma channel.

The longitudinal field created by the driving positron bunch is the convolution of the beam current ρ with the single-particle wake function

$$E_z(\xi) = \int_\xi^\infty \rho(\xi') W_z(\xi - \xi') d\xi'. \qquad (9)$$

The two-bunch current profile is assumed to be the superposition of two gaussian profiles.

We are now in a position to compare our analytic theory to numerical simulations. Figure 3 shows a QuickPIC [12] simulation of a positron drive and witness beam propagating to the right in a hollow plasma channel. The parameters of the simulation are similar to those used in the experiment, except for the charge of the witness bunch which is 1.5×10^9 in the simulation. The predicted longitudinal field (solid red
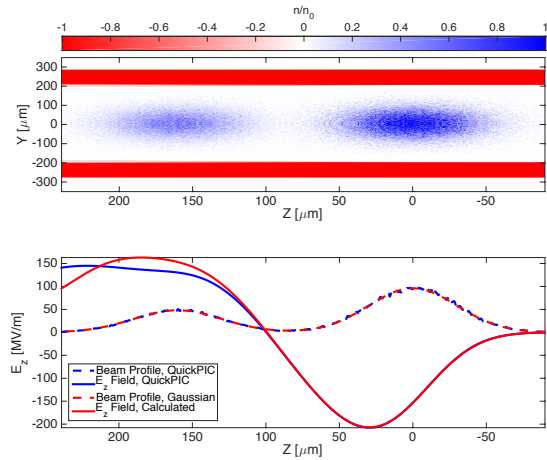

Figure 3: Top: A particle-in-cell simulation of a positron drive and witness beam propagating to the right in a hollow channel plasma using the code QuickPIC. Bottom: The simulated beam current is shown with a blue dashed line. The simulated current is approximated by the sum of two gaussians (dashed red line) for the analytic calculation. The simulated (solid blue) and calculated (solid red) on-axis, longitudinal fields are plotted together. There is excellent agreement between the two curves up to a longitudinal value of $\xi = 125\,\mu\mathrm{m}$ where charge separation begins to occur at the channel wall.

line) is compared to the simulated field (solid blue line) and is found to be in excellent agreement up to a longitudinal value of $\xi = 125\,\mu\mathrm{m}$. The discrepancy between the calculated and simulated field occurs when there is significant charge separation at the inner wall of the plasma channel. The dielectric boundary condition is violated at this point and the model is no loner valid. Additional theoretical work is needed to develop a model that accommodates both the longitudinal modes sourced by charge separation in the wall of the channel and the transverse modes confined by the wall of the channel.

Note that this simulation shows a nearly flat wakefield over the witness bunch for a drive to witness charge ratio of 2:1. Flat wakefields are ideal for witness beam acceleration because they do not increase the energy spread of the bunch. In the experiments described here the charge ratio is closer to 10:1, implying that the wake is not flattened by the witness beam. Nevertheless, we do not observe any change in the energy spread of the witness bunch because it is very short and the net energy change is modest.

RASTER SCAN MEASUREMENT

Before attempting to accelerate a positron witness bunch in the wake of a positron drive bunch within a hollow channel plasma, it is critical to confirm that the plasma channel has the desired annular transverse profile. We use a single driving positron bunch to measure the shape of the
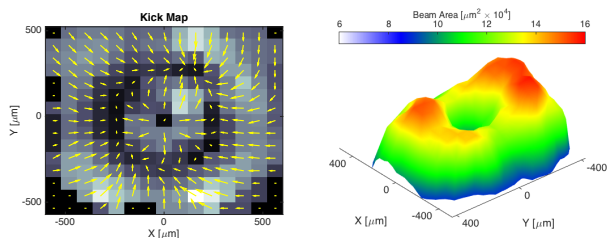
Figure 4: Left: A "kick-map" showing how the positron beam is deflected by nearby ionized regions. The arrows point to regions with plasma. Right: An "area-map" showing how the beam area increases on the downstream YAG screen due to the beam interacting with the wall of the plasma. Both the kick-map and area-map indicate some asymmetry in the channel.
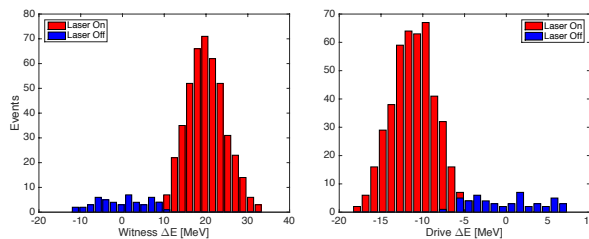

Figure 5: Left: The energy gain histogram for the witness bunch. The average energy gain is 19.9 MeV and the highest energy event is 33.4 MeV. Right: The energy loss histogram for the drive bunch. The average energy loss is 11 MeV. Note that in for this data, we operated with a 10 Hz positron beam and a 9 Hz laser, so that one out of every ten shots is a no-plasma background reference. There are 500 total shots in this dataset.

plasma channel using a technique we refer to as the "raster scan" [13].

For small displacements of the beam from the center of the channel, the beam induces a dipole deflecting mode that kicks the back of the bunch away from the channel center. We exploit this deflecting mode to study the shape of the channel by rastering the position of the laser relative to the positron beam. The laser trajectory is set by the position of the kinoform, which is mounted on a stage that can be actuated horizontally and vertically. We use the stage to raster the laser in the transverse plane while keeping the pointing of the laser parallel to the beam. The ionized plasma delivers a kick to the beam when the beam is off center in the channel, and this kick is recorded on a scintillating YAG screen 1.95 meters downstream of the interaction region (see Figure 1).

The results of the raster scan are shown in Figure 4. We create a "kick-map" that indicates the direction of beam deflection depending on its position relative to the channel. The shape of the kick map is consistent with our expectations for an annular ionized region. When the beam is outside the channel, the kicks point radially inwards toward the ionized region. When the beam is inside the channel, the kicks point radially outward toward the walls of the channel. The transverse wakefield increases in strength longitudinally throughout the bunch. Particles towards the back of the bunch see a larger kick than particles in the front. The beam profile stretches in the direction of the kick, and the beam area increases as a result. This is shown in the right sub-plot of Figure 4. The largest beam area growth occurs when the beam propagates along or through the ionized annulus. Both the kick map and beam area map show an annular feature with some asymmetry, which may be attributed to variations in the laser intensity around the first maximum of the Bessel profile, resulting in uneven ionization of the plasma annulus.

OBSERVATION OF ACCELERATION

Using our collimation system, we created a positron drive and witness beam with 1.6×10^9 and 1.6×10^8 particles/bunch, respectively. Using a deflecting cavity and

electro-optical sampling, we measured the drive bunch to be 50 μm long and the witness bunch to be less than 20 μm long (the resolution of the system). The bunch separation between the drive and witness beam varies from 100 to 300 μm. We observe acceleration of the witness bunch when the bunch spacing is 250 μm, which is longer than the ~150 μm spacing expected from particle-in-cell simulations.

The energy changes that we observe are small compared to the incoming energy spread and energy jitter. Therefore, we need to correct for both the incoming energy jitter and orbital correlations that can effect the energy measurement. As mentioned above, the imaging spectrometer is set such that R_{34} is close to zero. A small energy-orbit correlation was observed in the y-plane, at the level of 8 MeV/mm, which is corrected for on a shot-to-shot basis. Orbital variations were on the order of 10–100 μm.

The incoming beam energy jitter is greater than 10 MeV. In previous work, we used a simple technique where we matched the upstream and downstream dispersion in order to measure changes to the beam energy centroid [13]. In that case, we only used a single bunch and the dispersion matching procedure was sufficient to resolve changes in the beam energy. Here, the bunch energy spread is much larger than in the previous work due to the chirp needed for two-bunch collimation. Non-linear dispersion in the upstream spectrometer necessitates a more advanced energy correction technique. During the experiment, we operate with a 10 Hz positron beam and a 9 Hz laser. We record the 500 shots of the dataset, and compare the 450 shots with laser (plasma channel present) to shots without laser (no plasma). The 50 laser-off shots are sufficient to characterize all variations in the incoming energy spectra. After the upstream spectra are compared and matched, we use the matched laser-on spectra to predict the unperturbed spectra at the downstream spectrometer. We compare the measured laser-on spectrum to the matched laser-off spectrum in order to infer changes to the drive and witness beam energy.

Figure 5 shows the energy gain and energy loss of the witness and drive bunches, respectively. The witness bunch,
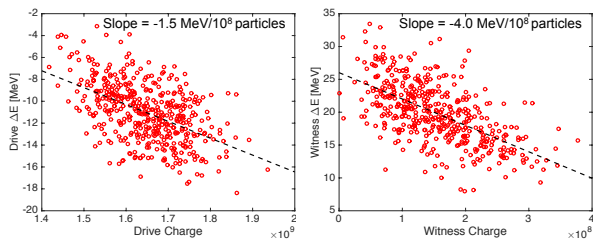
Figure 6: Left: The energy loss of the drive beam as a function of charge in the drive beam. The slope is $-1.5\,\text{MeV}/10^8$ particles. Right: The energy gain of the witness beam as a function of charge in the witness beam. The slope is $-4.0\,\text{MeV}/10^8$ particles. Assuming a linear wakefield and a drive beam with constant bunch length. We can infer that the beam loading effect due to the witness beam alone is $-2.5\,\text{MeV}/10^8$ particles.

with just one-tenth the charge of the drive bunch, experiences an accelerating field that is nearly twice as large as the drive bunch. The average acceleration of the witness beam is 19.9 MeV over the 25-cm long channel, and the average deceleration of the drive bunch is only 11 MeV over the same length. The transformer ratio is 1.8. This is the first demonstration of high transformer ratio PWFA for a drive-witness setup.

We also observe a very strong beam-loading effect where the acceleration of the witness bunch is reduced by increasing the charge of the witness bunch. Figure 6 shows the effect for both the drive and the witness beams. Increasing the drive beam charge increases the strength of the wake which in turn decelerates the drive bunch. Increasing the witness bunch charge loads the wake, and as a result, the net accelerating field is decreased. Note that in this experiment, the charge in the drive and witness beam are not independently tuned (*i.e.* more charge in the drive bunch implies less charge in the witness bunch and vice-versa). We are able to distinguish the beam loading effect from changes in wake amplitude by noting that the energy loss of the driver and the energy gain of the witness change at different rates with the respect to their bunch charge. Assuming that the drive bunch length does not change significantly with bunch charge, we can infer by superposition that the beam loading effect due to the witness beam alone is -2.5 MeV/10^8 particles.

The highest energy-gain shot in this dataset is 33.4 MeV, observed for a very low-charge witness beam with 5×10^7 particles, or one twentieth of the drive beam charge. The accelerating gradient for this shot is 133 MeV/m.

CONCLUSION

We have demonstrated, for the first time, the acceleration of a positron witness bunch in a hollow channel plasma. This technique may be used in future experiments to demonstrate staged acceleration of positrons, as well as the acceleration

of positrons in the wake of an electron drive beam. Such experiments will be possible at FACET-II. Both of these capabilities are critical for developing positron acceleration in plasma for a high-energy collider.

ACKNOWLEDGMENT

REFERENCES

[1] T.C. Chiou *et al.*, Laser wakefield acceleration and optical guiding in a hollow plasma channel. *Physics of Plasmas*, 2(1), 310-318, 1 (1995).

[2] T.C. Chiou and T. Katsouleas, High Beam Quality and Efficiency in Plasma-Based Accelerators. *Physical Review Letters*, 81(16), 3411-3414, 10 (1998).

[3] C.B. Schroeder *et al.*, Multimode Analysis of the Hollow Plasma Channel Wakefield Accelerator. *Physical Review Letters*, 82(6), 1177-1180, 2 (1999).

[4] M.J. Hogan *et al.*, Plasma wakefield acceleration experiments at FACET. *New Journal of Physics*, 12(5), 055030, 5 (2010).

[5] P. Muggli *et al.*, Photo-ionized lithium source for plasma accelerator applications. *IEEE Transactions on Plasma Science*, 27(3), 791-799, 6 (1999).

[6] S.Z. Green *et al.*, Laser ionized preformed plasma at FACET. *Plasma Physics and Controlled Fusion*, 56(8), 084011, 8 (2014).

[7] W.D. Kimura *et al.*, Hollow plasma channel for positron plasma wakefield acceleration. *Physical Review Special Topics - Accelerators and Beams*, 14(4), 041301, 4 (2011).

[8] N.E. Andreev *et al.*, Formation of high-power hollow Bessel light beams. *Quantum Electronics*, 26(2), 126-130, 2 (1996).

[9] J. Fan *et al.*, Tubular plasma generation with a high-power hollow Bessel beam. *Physical Review E*, 62(6), 7603-7606, 12 (2000).

[10] M. Litos *et al.*, High-efficiency acceleration of an electron beam in a plasma wakefield accelerator. *Nature*, 515(7525), 92-95, 11 (2014).

[11] A. Chao. *Physics of Collective Beam Instabilities in High Energy Accelerators.* Chapter 2. Wiley, (1993).

[12] W. An *et al.*, An improved iteration loop for the three dimensional quasi-static particle-in-cell algorithm: QuickPIC. *Journal of Computational Physics*, 250, 165-177, 10 (2013).

[13] S. Gessner *et al.*, Demonstration of the Hollow Channel Plasma Wakefield Accelerator. *Nature Communications*, in press (2016).